



ARTICLE

Kinetic Modeling of Light Naphtha Hydroisomerization in an Industrial Universal Oil Products Penex™ Unit

Ramzy S. Hamied¹, Zaidoon M. Shakor^{2,*}, Anfal H. Sadeiq¹, Adnan A. Abdul Razak² and Ammar T. Khadim³

¹Department of Petroleum Technology, University of Technology, Baghdad, Iraq

²Department of Chemical Engineering, University of Technology, Baghdad, Iraq

³Midland Refineries Company, Al-Dura Refinery, Baghdad, Iraq

*Corresponding Author: Zaidoon M. Shakor. Email: zaidoon.m.shakor@uotechnology.edu.iq

Received: 18 December 2022 Accepted: 13 February 2023

ABSTRACT

Recently, the isomerization of light naphtha has been increasingly significant in assisting refiners in meeting sternness specifications for gasoline. Isomerization process provides refiners with the advantage of reducing sulfur, olefin, and benzene in the gasoline basin without significantly victimizing the octane. The mathematical modeling of a chemical reaction is a critical tool due to it can be used to optimize the experimental data to estimate the optimum operating conditions for industrial reactors. This paper describes light naphtha isomerization reactions over a Pt/Al₂O₃-Cl catalyst at the Al-Dura Oil Refinery (Baghdad, Iraq) using a newly developed universal mathematical model. The proposed kinetic model involves 117 isomerization reactions and 90 cracking reactions to describe 52 real components graded from methane to n-octane. A Genetic Algorithm stochastic optimization technique applied in MATLAB R2020a software was employed to estimate the optimal set of kinetic parameters. The calculated activation energies for hydrocracking reactions was found to be higher than the other reactions because of hydrocracking reactions occur at higher range of temperatures. By benchmarking between the experimental and theoretical results for all 117 data sets, the mean absolute error was obtained to be 0.00360 for all 52 components. Also, a positive effect of increasing reaction temperatures was recognized on enhancing the research octane number (RON).

KEYWORDS

Light naphtha; hydroisomerization; reactions; kinetics; mathematical modelling

1 Introduction

The isomerization process works well for production high-quality gasoline by offering economic interest during the gasoline production with minimizing harmful gas emissions and high octane number [1,2]. The isomerization process is cost-efficient and plain for the enhancement of octane numbers in analogy to other processes enhancement of the octane. The isomerized light naphtha includes low level of benzene and sulfur, which makes it an ideal mixture component for a gasoline blending process [3].

The Penex™ isomerization process was designing particularly for continuous light naphtha catalytic isomerization. The reactor temperatures are the key process variables in Penex™ isomerization.



This work is licensed under a Creative Commons Attribution 4.0 International License, which permits unrestricted use, distribution, and reproduction in any medium, provided the original work is properly cited.

Temperatures that are greater than what is required to maintain equilibrium can increase the amount of hydrocracking and also the carbon formation on the catalyst [4]. The Universal Oil Products Penex™ unit consists of two series reactors, the first reactor hydrogenated all the benzene rings in the light straight-run naphtha feed, and a few conversions of methyl cyclopentane (MCP) and cyclohexane (CH) to hexanes, as well as some hydrocracking, occur for heptane components to C3 and C4 [5].

Light naphtha isomerization unit designing and choosing the operating condition requires a precise reaction mathematical kinetic model to appreciate the product's composition [6]. In order to improvement gasoline octane numbers, refiners prefer that isomerization of the short-chain paraffin because they are not harmful to the environment pollution [7,8]. This reactions permits normal alkanes (C5/C6) conversion which have low octane number, to be converted into branched-alkanes to increase values of the octane number [9]. The octane number of isomer is higher than that for normal paraffins. The octane number is zero for n-heptane and 92.8 for 2, 2-Dimethylpentane [1]. Therefore, optimizing and choosing the operating conditions for isomerization unit of light naphtha requires high precise kinetic model reaction to appreciate the composition of products [10,11].

Within the past ten years, few studies have been conducted on kinetic models for the isomerization of n-alkanes [12–21]. The type of feedstock and operating conditions of the most significant studies are reported in Table 1.

Ghafari et al. [22] developed a dimensionless model for light naphtha isomerization in a three-phase trickle-bed reactor. It deems the fundamental process of isomerization reactions involving isomerization, hydrocracking, hydrogenation, and reactions implementation of accurate kinetic equations dimensionless and rate constants. The dynamics are assessed to look at the system behavior with divergence in the concentration of hydrogen in the feedstock. The compositions of isomers calculated with the suggested model are in confirmation simulation outcome got by experimental data.

Barkalov et al. [23] applied parallel optimization method to estimate the kinetic parameters of a complicated chemical reaction for the developed kinetic model which consists of 48 reactions stages. The kinetic parameters make it possible to develop a mathematical model of the process, which is in good agreement with industrial data.

Ahmed et al. [24] developed a detailed mathematical model for industrial naphtha isomerization reactor process based on data from the Baiji North Refinery (BNR, Iraq). They estimate the parameters kinetic of (36) chemical reactions involved in the kinetic model suggested. The optimal amounts of the kinetic parameters were calculated by reducing the summation of the squared errors between the experimental and predicted data. Their model was applied to assess and develop a new isomerization process in order to enhance the research the octane number and yield of the reactor.

Faskhutdinov et al. [25] studied the transformation of pentane and hexane fractions by using a three-reactor block in catalytic isomerization operation. They evolved a mathematical kinetic model for isomerization involving (102) parameters kinetic. Their kinetic model reliably dubs not only the kind of the compositions bends along the department of reactor, but also the downstream product of final composition for the last reactor. Therefore, kinetic model can be employ to permit determine the optimal catalyst amount, and sizing of the reactors within cascades and retrofit the reactor blocks of existing plants.

Enikeeva et al. [26] developed a mathematical model for the catalytic isomerization process of the C5/C6 by describing the chemical reactions inside the reactors. They propose a mathematical description of optimization criteria for their model. The problem of multi-criteria optimization of the reactor block of the process is solved based on the developed mathematical model.

Table 1: Feedstock and operating conditions of the previous studies

Feed	WHSV (h ⁻¹)	H ₂ /Feed (molar)	Catalyst	T (°C)	P (bar)	Yield	Ref.
Palmitic acid	16	–	Pt/H-beta	285	40	42	[1]
C15–C18	1	30	Pt-HY	310	34	34	[4]
n-C16	2	–	Pt–Al-MCM-41	350	103	40	[5]
Hexane	6	2	Pt/MWCNT	350	1.013	72.7	[6]
Light naphtha	0.2–1.0	2–3	Pt-Zr/SiO ₂	450	13	–	[7]
<i>n</i> -hexadecane	1.1	10.9	Pt/ZSM-12	295	60	80	[9]
Pentane–hexane	–	–	Pt/SO ₄ -ZrO ₂	130	3	81	[13]
C5/C6	1.0–2.0	0.1–2.0	Pt-chlorinated alumina	120–180	20–30	99	[14]
n-butane	6–10	0.06–0.1	Sulfated oxide	180–200	15	–	[15]
Light straight	1.0–3.0	1.0–2.0	Chloride alumina	130–150	15–35	89	[27]
C7 + hydrocarbons	1.5–2.0	1.0–2.0	H-ZSM 5	160–200	10–20	–	[28]
Light naphtha	1.26	0.2	Pt/Al ₂ O ₃ -Cl	150	34	82.7	[29]
Light naphtha	0.9–2.0	1.2–2.0	Pt/Zeolite	200–260	25	–	[30]

A new universal kinetic model of 207 reactions was developed by Shakor et al. [4], they used experimental data obtained from previous studies for light naphtha isomerization over three different Pt/zeolite zeolites in pilot plant. The obtained kinetic model was valid within the temperature range 290°C to 390°C.

The operating conditions of industrial processes are different from the operating conditions of laboratory units, the catalyst works for longer periods in the industrial systems, as well as it exposed to extreme conditions. This study aims to estimate the kinetic parameters of newly developed kinetic model which depending on the data obtained from industrial Isomerization process.

2 Data Collection and Catalysts for Light Paraffin (C5/C6) Isomerization

Experimental data was collected from a light naphtha isomerization process located in Al-Dura Oil Refinery (Baghdad, Iraq). The collected data were the feed composition and reactor effluent at different temperatures. Pt/chlorinated Al₂O₃ catalysts were used in the isomerization process, where the operating conditions for the process were: temperatures in the range of 120°C–180°C, total pressure = 3.0–4.0 MPa; weight of the catalyst = 32.6 g; liquid hourly velocity (LHSV [h⁻¹]) = 1.5 h⁻¹; and mole ratio H₂:HC = (0.3–0.5):1. Table 2 summarizes the physical properties of the components used in this study.

Table 2: Physical properties of the components

No.	Methyl	Formula	Mole. Wt.	Normal boiling point °C	Specific gravity 15.55/ 15.55	Ideal gas Cp @ 15.55°C KJ/Kg	Liquid Cp @ 15.55°C KJ/Kg	Ideal gas heat of formation @ 25°C KJ/Kg	Octane number, research, clear
1	PROPANE	C ₃ H ₈	44.10	-6.52	0.5070	0.9036	1.4421	-2373.93	1.8
2	ISOBUTANE	C ₄ H ₁₀	58.12	-11.78	0.5629	0.8994	1.3274	-2322.60	102.0
3	N-BUTANE	C ₄ H ₁₀	58.12	-0.511	0.5840	0.9187	1.3260	-2161.83	94.0
4	ISOPENTANE	C ₅ H ₁₂	72.15	27.84	0.6247	0.8941	1.2509	-2130.29	92.0
5	N-PENTANE	C ₅ H ₁₂	72.15	36.06	0.6311	0.9029	1.2641	-2033.43	62.0
6	2,2-DIMETHYLBUTANE	C ₆ H ₁₄	86.18	49.73	0.6535	0.8871	1.1948	-2142.96	91.8
7	CYCLOPENTANE	C ₅ H ₁₀	70.13	49.26	0.7603	0.6308	0.9832	-1101.33	100.1
8	2,3-DIMETHYLBUTANE	C ₆ H ₁₄	86.18	57.98	0.6670	0.8715	1.1955	-2051.50	105.8
9	2-METHYLPENTANE	C ₆ H ₁₄	86.18	60.26	0.6578	0.8957	1.2248	-2027.04	76.0
10	3-METHYLPENTANE	C ₆ H ₁₄	86.18	63.28	0.6689	0.8845	1.2067	-1996.52	76.0
11	N-HEXANE	C ₆ H ₁₄	86.18	68.73	0.6638	0.8985	1.2369	-1937.21	24.8
12	METHYLCYCLOPENTANE	C ₆ H ₁₂	84.16	71.81	0.7540	0.6980	1.0243	-1267.74	91.3
13	2,2,3-TRIMETHYLPENTANE	C ₈ H ₁₈	114.23	109.84	0.7202	0.8836	1.1692	-1925.53	105.0
14	BENZENE	C ₆ H ₆	78.11	80.10	0.8829	0.5598	0.9550	1061.72	102.7
15	CYCLOHEXANE	C ₆ H ₁₂	84.16	80.73	0.7835	0.6726	1.0004	-1463.10	82.5
16	2-METHYLHEXANE	C ₇ H ₁₆	100.20	90.05	0.6823	0.8852	1.2137	-1943.28	52.0
17	3-METHYLHEXANE	C ₇ H ₁₆	100.20	91.85	0.6928	0.8808	1.2009	-1909.46	52.0
18	METHYLCYCLOHEXANE	C ₇ H ₁₄	98.19	100.93	0.7748	0.7394	1.0232	-1576.19	74.8
19	1-HEPTENE	C ₇ H ₁₄	98.19	93.64	0.7015	0.8557	1.1878	-634.48	54.5
20	N-HEPTANE	C ₇ H ₁₆	100.20	98.42	0.6882	0.8943	1.2292	-1872.73	0.0
21	N-OCTANE	C ₈ H ₁₈	114.23	125.67	0.7070	0.8915	1.2183	-1828.09	-15.0

Isomerization processes consist of three types: (1) low-temperature reactions (120°C–180°C) are utilized for chlorinated alumina, (2) medium reactions temperature range (250°C–300°C) have been informed by using zeolites, and (3) high reaction temperature between (360°C–440°C) are promoted generally by fluorinated alumina [27]. The catalysts used in this work are employed widely in industrial operations at 130°C–180°C because these catalysts are based on chlorinated alumina [31]. Chlorinated alumina catalysts are the most active and provide the greatest yield of iso-alkanes, thus producing the highest octane number isomers. Because of the gradual reduction of the acidity in the isomerization catalyst during the process (which decreases the isomerization activity), these reactions require the addition of alkyl chlorides to the feed. Alkyl chlorides need to be removed because the reactor is affected by the deposition of some products from these. Additional problems comprise high allergy to sulfur, benzene, water, and nitrogen, which make the catalysts poison. The process is more costly because of the feedstock's necessity to be purified.

3 Mechanism of the Isomerization Process for Light Naphtha (C5/C6)

Hydroisomerization reaction occurs consecutively when normal alkane is dehydrogenated firstly to alkene onto a metal site in the isomerization operation onto bifunctional acid catalysis. Next, the ion carbenium, which in turn is isomerized onto an acidic site to create an iso-olefin through isocarbo-cation, lastly forms bi alkanes or multi branched alkanes [32,33]. Alkylcarbenium ions can

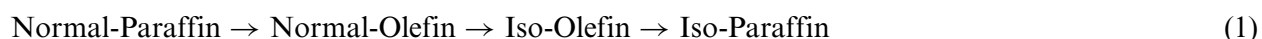
then undergo a β -scission reaction [34], forming cracking products. The isomerization industrial process feedstock is light straight-run naphtha (range of the boiling 27°C – 70°C) and is mainly a form of normal paraffin, normal pentane, and normal hexane.

Analyzing the composition of the product and the feed is necessary to obtain the formalized reaction scheme of the industrial isomerization process. The light naphtha industrial isomerization process generally occurs on bifunctional catalysts consisting of acid sites for skeletal isomerization and metallic sites for hydrogenation/dehydrogenation.

There are three stages for isomerization reaction:

1. Disposal of normal paraffin molecules on the location of the dehydrogenation and hydrogenation which results in normal olefin dehydrogenation.
2. Disposal of normal paraffin from dehydrogenation sites and releasing it to places with regular structure that changes olefins to iso-olefins.
3. Dehydrogenation of iso-olefin molecules to iso-paraffin.

Dehydrogenation of normal paraffin generally can be conducted during the bi-function below [35,36]:



The isomerization process mathematical model is a valuable tool in the crude oil refining industry because the isomerization process of light naphtha is a complex chemical reaction network where some kinds of reactions find on metal catalyst sites vs. acid sites [37,38]. This means that laboratories must change the parameters they employ as the basis for process optimization in commercial reactors. Fig. 1 shows a schematic of the PenexTM isomerization unit.

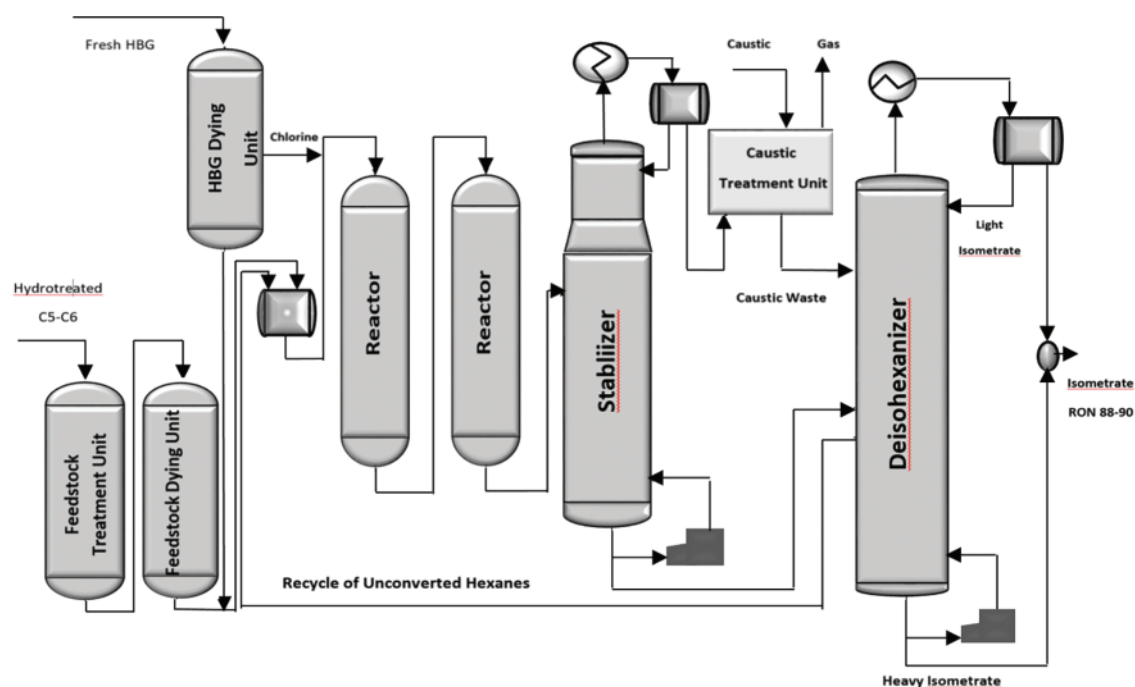


Figure 1: Schematic of PenexTM isomerization unit [39]

4 Mathematical Modeling of the Penex™ Isomerization Process

The initial mathematical model step characterization of the subject is to build scheme reactions for hydrocarbon during the isomerization process [15]. The mathematical model assumptions were considered as the following [39–43]:

- Steady state non-isothermal reactor conditions [39].
- All reactions were happening in gas phase [40].
- One-dimensional plug flow in the reactor [23].
- The first-order pseudo reactions with respect to hydrocarbons [41,42].

The description of the mathematical model of the hydrocarbon feedstock catalytic isomerization operation is setup onto heat balances and properties component-wise material [43]:

$$G \cdot \frac{dC_i}{dz} + G \cdot \frac{dC_i}{dV} = \sum_{j=1}^m a_j \cdot r_j \quad (2)$$

$$G \cdot \frac{dT}{dz} + G \cdot \frac{dT}{dV} = \frac{1}{\rho \cdot C_p} \sum_{j=1}^m a_j \cdot r_j \cdot \Delta h_j \quad (3)$$

If the $r = 0$, $C = CO$; if $Z = 0$, $C = 0$; if $r = 0$, $T = T_{in}$; if $Z = 0$, $T = T_0$

where G is a flow rate of feedstock (m^3/h); C_i is the i^{th} component concentration ($mole/m^3$); V is a volume of catalyst bed (m^3); a is the activity of catalyst; ρ is the hydrocarbon mixture density (kg/m^3); C_p is heat capacity of the hydrocarbon mixture [$J/(kg \cdot K)$] and $z = t \cdot G$ (t is the total time of working catalyst starting from the new loading catalyst [h]).

The reaction rate equation is expressed in terms of the partial pressures of the reaction components, as shown in Eq. (3). The reaction in gaseous phase can be represented as a function of molar concentration C_i where $C_i = P_i^0/(R \cdot T)$. All reactions took place in a gaseous phase at higher temperatures during the isomerization process [44]:

$$r_j = k_j P_i^0 \quad (4)$$

An Arrhenius equation (Eq. (5)) was used to represent the divergence in constants rate of reaction with activation energy and temperature:

$$k_j = k_j^0 \exp\left(-\frac{E_{A_j}}{RT}\right) \quad (5)$$

where the partial pressure is P_i (bar), the constant of the gas is R is 8.314 ($J/mole \cdot ^\circ K$), the activation energy is E_A ($J/mole$), the pre-exponential factor is A ($mole/gm.cat.hr \cdot bar$), and the temperature is T ($^\circ K$).

4.1 Estimation of Kinetic Model Parameters

To minimize the objective function (f) is used the differential evaluation-optimization algorithm, which represents the compositions of the reactors effluents deviations in order to estimate the global optimum set of parameters kinetic.

$$f = \frac{\sum_{i=1}^{n_{exp}} \sum_{j=1}^{n_{com}} |y_{ij}^{exp} - y_{ij}^{pred}|}{n_{exp} \times n_{com}} \quad (6)$$

The light naphtha isomerization process of the proposed mathematical model of over the Pt/chlorinated Al_2O_3 involved 53 equations of ordinary differential (52 for components of light

naphtha and one for hydrogen). These differential equations were solved using the fourth-order Runge-Kutta integration method, represented in Eq. (2). MATLAB R2020a software program coding was used for all computations. The optimization method of genetic algorithm was employed to estimate the optimum group of parameters kinetic. The integration and optimization calculation used the MATLAB sub-routines **ode15s** and **ga**. Table 3 shows all of the estimated pre-exponential factors values of the (A1–A207) and the activation energies (E1–E207).

Table 3: Estimated reaction kinetic parameter

Isomerization reactions	Pre-exponential factor (m ³ /mol.s)	Activation energy (j/mol)	Hydrogenation reactions	Pre-exponential factor (m ³ /mol.s)	Activation energy (j/mol)
n – C₄ → i – C₄	1.3100	146501.6	i – C₄ + H₂ → C₃ + C₁	0.3310	271861.4
i – C₄ → n – C₄	3.6258	22525.9	i – C₄ + H₂ → 2C₂	0.6377	119466.8
n – C₅ → i – C₅	1.2080	25618.2	n – C₄ + H₂ → C₃ + C₁	0.3677	88107.49
i – C₅ → n – C₅	0.2335	35625.1	n – C₄ + H₂ → 2C₂	93.4306	24801.97
n – C₅ → CP + H₂	0.5977	157695.3	i – C₅ + H₂ → i – C₄ + C₁	0.0556	35055.04
CP + H₂ → n – C₅	15.7977	21962.0	i – C₅ + H₂ → n – C₄ + C₁	2.4414	97357.91
MCP + H₂ → 2 – MP	0.0345	26496.9	i – C₅ + H₂ → C₃ + C₂	0.3202	138297.4
MCP + H₂ → 3 – MP	1.3192	27253.2	n – C₅ + H₂ → n – C₄ + C₁	2.1942	27221.09
MCP → CH	0.8130	26136.0	n – C₅ + H₂ → C₃ + C₂	0.4073	250880.9
CH → MCP	1.3568	35435.3	2, 2 – DMB + H₂ → i – C₅ + C₁	0.3491	67833.47
B + 3H₂ → MCP	7.4851	29466.8	2, 2 – DMB + H₂ → 2C₃	0.2400	168392.6
MCP → B + 3H₂	0.1621	222705.8	2, 3 – DMB + H₂ → i – C₅ + C₁	0.6502	39482.95
B + 3H₂ → CH	3.7888	22895.9	2, 3 – DMB + H₂ → 2C₃	0.5570	294989.8
CH → B + 3H₂	0.7347	191618.2	2 – MP + H₂ → i – C₅ + C₁	0.9577	36495.53
CH + H₂ → n – C₆	1.4380	26393.7	2 – MP + H₂ → i – C₄ + C₂	3.0713	51328.19
n – C₆ → CH + H₂	1.7833	195269.3	2 – MP + H₂ → 2C₃	0.2212	232013.7
n – C₆ → 2 – MP	0.6682	24673.5	3 – MP + H₂ → i – C₅ + C₁	0.0257	67644.76

(Continued)

Table 3 (continued)

Isomerization reactions	Pre-exponential factor (m ³ /mol.s)	Activation energy (j/mol)	Hydrogenation reactions	Pre-exponential factor (m ³ /mol.s)	Activation energy (j/mol)
2 – MP → n – C₆	0.6991	27148.7	3 – MP + H₂ → n – C₅ + C₁	0.3787	33973.7
n – C₆ → 3 – MP	1.5561	26188.1	3 – MP + H₂ → n – C₄ + C₂	1.0565	40312.66
3 – MP → n – C₆	0.0310	54810.4	n – C₆ + H₂ → n – C₄ + C₂	0.1065	106689.8
2 – MP → 2,2 – DMB	0.8184	217528.0	n – C₆ + H₂ → n – C₅ + C₁	1.7031	33311.71
2,2 – DMB → 2 – MP	1.9917	70965.8	n – C₆ + H₂ → 2C₃	0.8366	153891.9
3 – MP → 2,2 – DMB	0.7103	21369.8	2 – MH + H₂ → n – C₆ + C₁	0.2561	203587.7
2,2 – DMB → 3 – MP	0.7449	42907.9	2 – MH + H₂ → 2 – MP + C₁	2.0737	268447.8
2 – MP → 2,3 – DMB	1.0398	172050.9	2 – MH + H₂ → i – C₄ + C₃	0.9260	175440.3
2,3 – DMB → 2 – MP	5.6961	42044.4	3 – MH + H₂ → n – C₆ + C₁	0.0978	114993.1
3 – MP → 2,3 – DMB	21.6776	52337.7	3 – MH + H₂ → 3 – MP + C₁	0.2881	248772.2
2,3 – DMB → 3 – MP	0.7024	29896.9	3 – MH + H₂ → i – C₅ + C₂	0.3741	110287.2
2 – MP → 3 – MP	1.0170	28629.4	3 – MH + H₂ → n – C₄ + C₃	0.4375	191666.7
3 – MP → 2 – MP	1.0759	51225.6	n – C₇ + H₂ → n – C₄ + C₃	0.3411	147101.8
MCH + H₂ → n – C₇	0.5280	239651.3	n – C₇ + H₂ → n – C₅ + C₂	0.3661	144324.9
n – C₇ → MCH + H₂	0.2633	20568.3	n – C₇ + H₂ → n – C₆ + C₁	0.7376	220612.3
n – C₇ → 2 – MH	0.9124	203644.7	n – C₈ + H₂ → n – C₇ + C₁	23.0498	21501.66
2 – MH → n – C₇	0.0044	59222.0	n – C₈ + H₂ → n – C₆ + C₂	0.2194	132848.9
n – C₇ → 3 – MH	3.2590	27889.5	n – C₈ + H₂ → n – C₅ + C₃	0.4206	125990.9
3 – MH → n – C₇	0.7915	195412.4	n – C₈ + H₂ → 2n – C₄	0.0271	217741.6

(Continued)

Table 3 (continued)

Isomerization reactions	Pre-exponential factor (m ³ /mol.s)	Activation energy (j/mol)	Hydrogenation reactions	Pre-exponential factor (m ³ /mol.s)	Activation energy (j/mol)
n – C₇ → C7 = +H₂	2.9437	24469.5			
C7 = +H₂ → n – C₇	0.5593	187510.3			
MCH + H₂ → 2 – MH	0.2246	142782.0			
MCH + H₂ → 3 – MH	0.4390	196173.6			
n – C₈ → 2, 2, 3 TMP	0.2981	225344.6			
2, 2, 3 TMP → n – C₈	15.8461	21871.18			

4.2 Estimation Isomerization Research Octane Number

Nikolaou et al. [45] developed a new method to estimate research octane number for gasoline, which simulates the RON for the reaction products. When calculating the total blended RON in this method the influence of the individual hydrocarbon products is taken into account which based on Eq. (7) [46]:

$$\text{RON} = \sum_{i=1}^{nc} x_i \times \text{RON}_i \quad (7)$$

where x_i is the i th component weight fraction, i presents in the isomerization product, and research octane number (RON_i) is the RON of the i component.

5 Results and Discussion

Evaluation of the proposed mathematical model of the industrial isomerization process compared the experimental and predicted mole fraction for all 117 data sets of isomerization products shown in Fig. 2. Comparing the predicted and experimental mole fractions was very small absolute error because the clusters points around the diametrical line confirmed the proper for proposed mathematical model. This means there was good agreement between the theoretical and industrial results for all 117 data sets of the isomerization products, where the absolute mean error for the Pt/Al₂O₃-Cl catalysts was 0.00360 for all component compositions at various temperatures. This compares favorably to Hayati et al. [28], who found that the absolute error (the difference summation among the calculated and experimental worth of the parts mole portions) of the light naphtha isomerization process was about 4.27%.

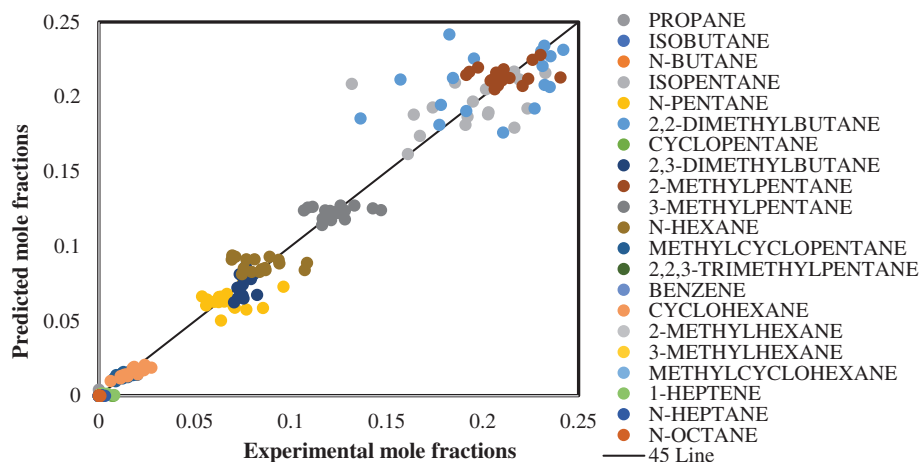


Figure 2: Comparison between the experimental and predicted mole fractions of isomerization

Fig. 3 demonstrates that the absolute error between the actual and simulated results for all components and data sets for the proposed mathematical model show an excellent agreement, indicated by low absolute error values. Also, the mean absolute error between the actual and simulated results for all the components shown in Fig. 4 agree very well, with the maximum mean absolute error value less than 0.025. In comparison, Faskhutdinov et al. [25] studied the pentane-hexane cut isomerization catalytic process; with estimated values to their most model components having no more than 5% error in comparison with the industrial data.

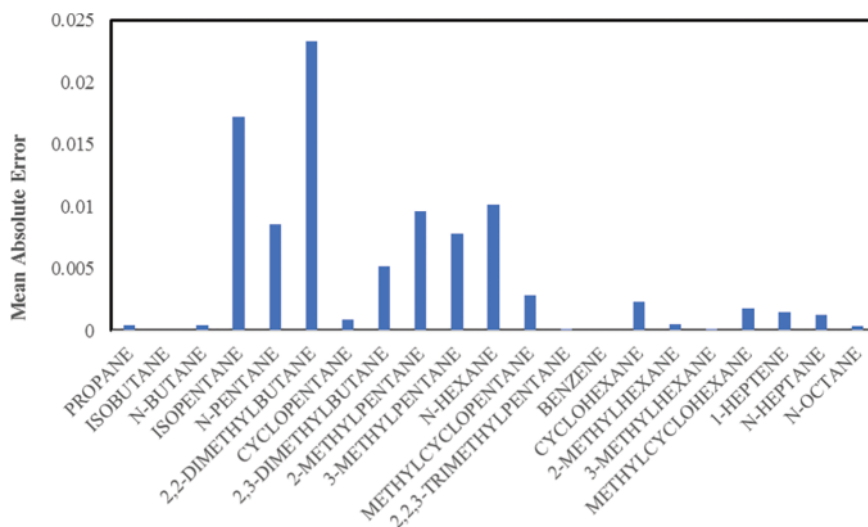


Figure 3: Comparison between the actual and predicted mole fractions of the isomerization products for all 117 data sets

The results in both Figs. 3 and 4 display smaller error values with increasing temperatures because the isomerization and cracking reactions are expected to occur at high temperatures. This factor is included in the proposed kinetic model and agrees with Shehata et al. [47].

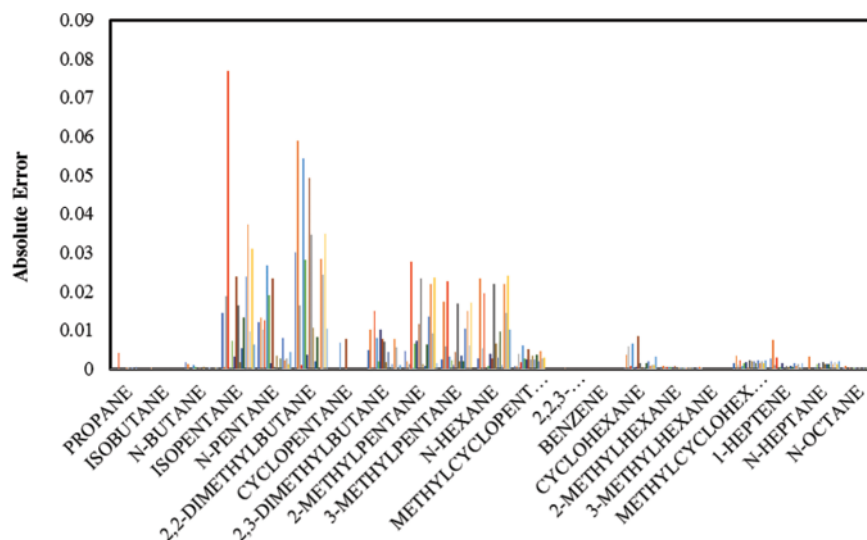


Figure 4: Absolute error between the actual and simulated results for all components and data sets

Activation energy values and pre-exponential factor were calculated according to the Arrhenius equation (Eq. (5)), and all results are shown in Table 3, which represents all of the kinetic reaction parameters of the reactor model for light naphtha in the industrial isomerization process. The hydrocracking reactions activation energy were greater compare with another reactions because at higher temperatures occurs of hydrocracking reactions. Linear alkanes in the isomerization process has a lower activation energy compared with the inverse reaction; which observed that linear alkanes have higher activity compared to inverse reactions in the isomerization reactions. In comparison with other studies, Ahmed et al. [24] and Dhar et al. [19] calculated the activation energy of the light naphtha kinetic model isomerization process, estimating the cracking reaction activation energy at a higher value than the isomerization reaction because increasing the temperature also causes the target and side reaction speed to rise.

Eq. (7) was used to estimate the influence of the feedstock temperature on the RON of the isomerizate (shown in Fig. 5) on the above based result. Increasing the temperature has a positive effect for research octane number when using a catalyst. It was expected that increasing the temperature (which relates to the properties thermodynamic of like these reactions and accelerates the incidence of hydrocracking) would lead to a decrease in the RON of the products. However, isomerization is a reversible reaction, which can imply going either from the left side to the right (n-Pentane into iso-Pentane) or from the right side to the left (iso-Pentane into n-Pentane). Lower temperatures favor the production of branched molecules, while high temperatures favor the production of normal straight-chain molecules (Valavarasu et al. [2] and Chekantsev et al. [44]). The species with higher octane numbers are turned into light specie, like butane, propane, and methane. Then separated light species from the product in the shape of fuel gas, and continually reduced the octane number unto hydrocracked the hydrocarbon containing six carbons species. However, as the temperature of the reaction increases, the RON increases because of the isomerization of the species resulting from reaction cracking of five atoms of carbon [47]. The hydrocracking reactions highly influence the RON, such that they can predominate over other reactions. Also, the resulting values of the RON for the proposed model agree with Awan et al. [48], who studied the Penex™ process for the isomerization of light naphtha.

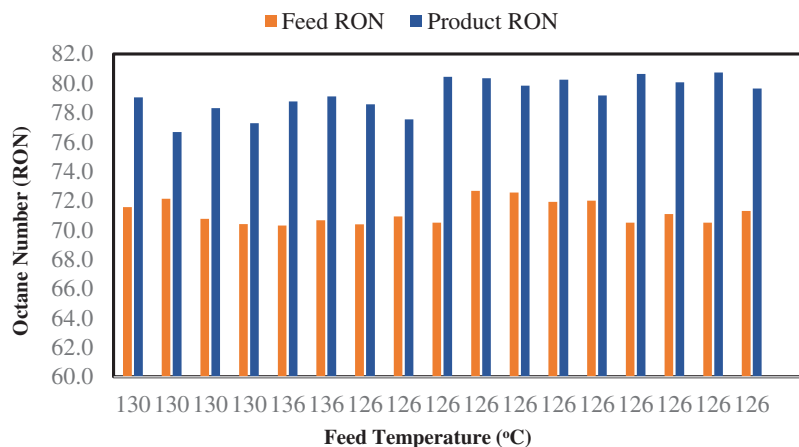


Figure 5: Effect of the feed RON and feed temperature on the products' RON

The model accuracy is rectifying by compare the experimental results together with model's prediction. Fig. 6 illustrates the compression between the research octane number for the measured and simulated products. There was good agreement between the values measured during the industrial isomerization process, which also agree with Chen et al. [49]. The simulated results for the proposed model have a maximum error value of less than 3%, which supports our aforementioned deductions.

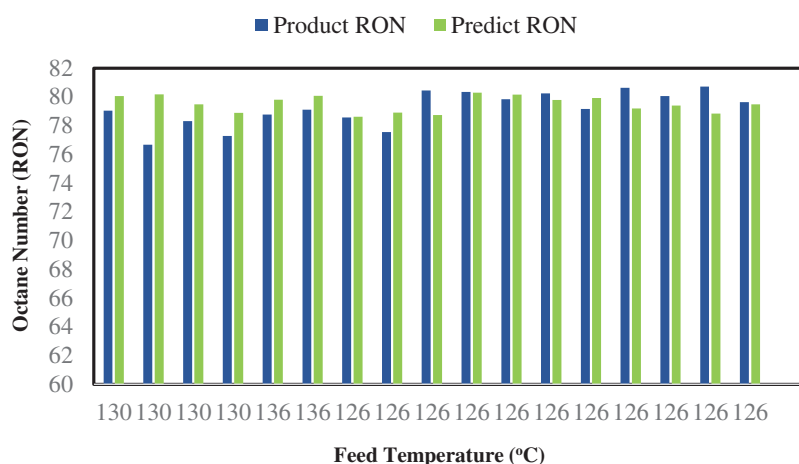


Figure 6: Comparisons between the RON of the measured and simulated products

6 Conclusions

The suitable kinetic model development depending on the reaction mechanism is a critical step in the mathematical model construction. Resolving the reverse kinetic issues authorizes parameters defining the render for the mathematical model as the bases and takes the consideration the aspects of chemical and physical process. The suggested mathematical model will support accurate predicted calculations, thereby allowing for the choice of the optimal technological conditions to ameliorate the adequacy resources for light naphtha isomerization process.. This work detailed the reactor block mathematical model of the Penex™ isomerization, characterize a kinetic reaction model of (52)

component and (207) reactions that explain the light naphtha isomerization reactions on catalysts (Pt/Al₂O₃-Cl). The predicted mole fraction products when compared with the experimental data shows an excellent agreement, with mean absolute error of (0.003608), using Pt/Al₂O₃-Cl catalysts for all 117 data sets of the isomerization products. The results of the hydrocracking reactions calculated for activation energy were greater compare with another because at higher temperatures occurs of hydrocracking reactions. Also, the temperature increase has a positive effect on the research octane number of the catalyst employed in the isomerization process of light naphtha.

Acknowledgement: The authors are thankful to the staff of the Petroleum Technology and Chemical Engineering Department-University of Technology-Iraq for supporting this work, also thankful Al-Dura Oil Refinery (Baghdad, Iraq).

Funding Statement: The authors received no specific funding for this study.

Conflicts of Interest: The authors declare that they have no known competing financial interests or personal relationships that could have appeared to influence the work reported in this paper.

References

1. Shakor, Z. M., María, J. R., Adnan, A. R. (2022). A detailed reaction kinetic model of light naphtha isomerization on Pt/zeolite catalyst. *Journal of King Saud University-Engineering Sciences*, 34(5), 303–308. <https://doi.org/10.1016/j.jksues.2020.12.006>
2. Valavarasu, G., Sairam, B. (2013). Light naphtha isomerization process: A review. *Journal of Petroleum Science and Technology*, 31(6), 580–595. <https://doi.org/10.1080/10916466.2010.504931>
3. Ghazizahedi, Z., Hayati-Ashtian, M. (2020). Retrofitting isomerization process using pinch analysis. *Journal of Energy Sources, Part A: Recovery, Utilization and Environmental Effects*. <https://doi.org/10.1080/15567036.2020.1859008>
4. Shakor, Z. M., AbdulRazak, A. A., Sukkar, K. A. (2020). A detailed reaction kinetic model of heavy naphtha reforming. *Arabian Journal for Science and Engineering*, 45(9), 7361–7370. <https://doi.org/10.1007/s13369-020-04376-y>
5. Hamied, R. S., Sukkar, K. A., Majdi, H. S., Shnain, Z. Y., Graish, M. S. et al. (2023). Catalytic-level identification of prepared Pt/HY, Pt-Zn/HY, and Pt-Rh/HY nanocatalysts on the reforming reactions of n-heptane. *Processes*, 11(1), 270. <https://doi.org/10.3390/pr11010270>
6. Fúnez, A., Lucas, A. D., Sánchez, P., Ramos, M. J., Valverde, J. L. (2008). Hydroisomerization in liquid phase of a refinery naphtha stream over Pt–Ni/H-beta zeolite catalysts. *Chemical Engineering Journal*, 136(2–3), 267–275. <https://doi.org/10.1016/j.cej.2007.03.062>
7. Kokkinos, N. C., Nikolaou, N., Psaroudakis, N., Mertis, K., Mitkidou, S. et al. (2015). Two-step conversion of LLCN olefins to strong anti-knocking alcohol mixtures catalysed by Rh, Ru/TPPTS complexes in aqueous media. *Catalysis Today*, 247(1), 132–138. <https://doi.org/10.1016/j.cattod.2014.07.058>
8. Kokkinos, N. C., Kazou, E., Lazaridou, A., Papadopoulos, C. E., Psaroudakis, N. et al. (2013). A potential refinery process of light-light naphtha olefins conversion to valuable oxygenated products in aqueous media–Part 1: Biphasic hydroformylation. *Fuel*, 104, 275–283. <https://doi.org/10.1016/j.fuel.2012.08.040>
9. Boda, L., Onyestyák, G., Solt, H., Lónyi, F., Valyon, J. et al. (2010). Catalytic hydroconversion of tricapyrlin and caprylic acid as model reaction for biofuel production from triglycerides. *Applied Catalysis A: General*, 374(1–2), 158–169. <https://doi.org/10.1016/j.apcata.2009.12.005>
10. Saginayev1, A., Tastanova, L., Apendina, A., Ishmukhanbetova, N., Dosmurzina, E. (2021). Hydro-catalytic isomerization of light gasoline fraction of Zhanazhol field's oil. *International Symposium "Sustainable Energy and Power Engineering 2021" (SUSE-2021)*, vol. 288, pp. 01021. <https://doi.org/10.1051/e3sconf/202128801021>

11. Mohammadrezaee, A., Kharat, A. N. (2018). Combined light naphtha isomerization and naphthenic ring opening reaction on modified platinum on chlorinated alumina catalyst. *Reaction Kinetics, Mechanisms and Catalysis*, 126(1), 513–528. <https://doi.org/10.1007/s11144-018-1490-1>
12. Khajah, M., Chehadeh, D. (2022). Modeling and active constrained optimization of C5/C6 isomerization via artificial neural networks. *Chemical Engineering Research and Design*, 182(3), 395–409. <https://doi.org/10.1016/j.cherd.2022.04.015>
13. Abdolkarimi, V., Sari, A., Shokri, S. (2022). Robust prediction and optimization of gasoline quality using data-driven adaptive modeling for a light naphtha isomerization reactor. *Fuel*, 328(15), 125304. <https://doi.org/10.1016/j.fuel.2022.125304>
14. Yang, C., Zheng, Z. (2022). Construction of a chemical kinetic model of five-component gasoline surrogates under lean conditions. *Molecules*, 27(3), 1080. <https://doi.org/10.3390/molecules27031080>
15. Kamel, S. A., Mohammed, W. T., Aljendeel, H. (2021). Synthesis and characterization of Ni-WO₃/sulfated zirconia nano catalyst for isomerization of N-hexane and Iraqi light naphtha. *Iraqi Journal of Chemical and Petroleum Engineering*, 22(4), 1–10. <https://doi.org/10.31699/IJCPE.2021.4.1>
16. Duchêne, P., Mencarelli, L., Pagot, A. (2020). Optimization approaches to the integrated system of catalytic reforming and isomerization processes in petroleum refinery. *Computers & Chemical Engineering*, 141(10), 107009. <https://doi.org/10.1016/j.compchemeng.2020.107009>
17. Faskhutdinova, R. I., Faskhutdinov, A. G., Enikeeva, L. V., Gubaydullin, I. M. (2021). Study of stiff differential equations of mathematical description of izomerization of pentane-hexane cut process. *Journal of Physics: Conference Series*, 22003. <https://doi.org/10.1088/1742-6596/2131/2/022003>
18. Irandoukht, A., Abbasi, A., Safaei, M. (2018). Octane number prediction in light naphtha isomerization plants. *Mechanics, Materials Science & Engineering*, 18. <https://doi.org/10.2412/mmse.29.36.874>
19. Dhar, A., Vekariya, R. L., Sharma, P. (2017). Kinetics and mechanistic study of *n*-alkane hydroisomerization reaction on Pt-doped γ -alumina catalyst. *Petroleum*, 3(4), 489–495. <https://doi.org/10.1016/j.petlm.2017.02.001>
20. Parsafard, N., Peyrovi, M. H., Rashidzadeh, M. (2016). Experimental and kinetic study of *n*-heptane isomerization on nanoporous Pt-Re, Sn/HPT/ZSM5-HMS catalysts. *Chinese Journal of Catalysis*, 37(9), 1477–1486. [https://doi.org/10.1016/S1872-2067\(15\)61114-7](https://doi.org/10.1016/S1872-2067(15)61114-7)
21. Chuzlova, C. A., Ivanchina, E. D., Dolganov, I. M., Igor, M., Molotov, K. I. (2015). Simulation of light naphtha isomerization process. *Procedia Chemistry*, 15, 282–287. <https://doi.org/10.1016/j.proche.2015.10.045>
22. Ghafari, S., Lay, E. N., Garshasbi, M. (2022). Development of a dimensionless and dynamic model of the three-phase trickle bed reactor in light naphtha isomerization process: Effects of axial mass dispersion and liquid-solid mass transfer on isomers concentration. *International Journal of Chemical Reactor Engineering*, 21(1), 109–128. <https://doi.org/10.1515/ijcre-2021-0274>
23. Barkalov, K., Gubaydullin, I., Kozinov, E., Lebedev, I., Faskhutdinova, R. et al. (2022). On solving the problem of finding kinetic parameters of catalytic isomerization of the pentane-hexane fraction using a parallel global search algorithm. *Mathematics*, 10(19), 3665. <https://doi.org/10.3390/math10193665>
24. Ahmed, A. M., Jarullah, A. T., Fayadh, M., Abed, F. M., Mujtaba, I. M. (2018). Modeling of an industrial naphtha isomerization reactor and development and assessment of a new isomerization process. *Chemical Engineering Research and Design*, 137, 33–46. <https://doi.org/10.1016/j.cherd.2018.06.033>
25. Faskhutdinov, A. G., Faskhutdinova, R. I., Arefyev, I. A., Enikeeva, L. V. (2019). Numerical simulation of the catalytic process of isomerization of pentane-hexane cut. *Journal of Physics: Conference Series*, 1368(4), 42016. <https://doi.org/10.1088/1742-6596/1368/4/042016>
26. Enikeeva, L. V., Faskhutdinov, A. G., Koledina, K. F., Faskhutdinova, R. I., Gubaydullin, I. M. (2021). Modeling and optimization of the catalytic isomerization of the pentane-hexane fraction with maximization of individual high-octane components yield. *Reaction Kinetics, Mechanisms and Catalysis*, 133(2), 879–895. <https://doi.org/10.1007/s11144-021-02020-w>

27. Naqvi, S. R., Bibi, A., Naqvi, M., Noor, T., Nizami, A. et al. (2018). New trends in improving gasoline quality and octane through naphtha isomerization: A short review. *Applied Petrochemical Research*, 8(3), 131–139. <https://doi.org/10.1007/s13203-018-0204-y>
28. Hayati, R., Abghari, S. Z., Sadighi, S., Bayat, M. (2015). Development of a rule to maximize the research octane number (RON) of the isomerization product from light naphtha. *Korean Journal of Chemical Engineering*, 32(4), 629–635. <https://doi.org/10.1007/s11814-014-0243-8>
29. Said, M. M., Ahmed, T. S., Moustafa, T. M. (2014). Predictive modeling and optimization for an industrial penex isomerization unit—A case study. *Energy Fuels*, 28(12), 7726–7741. <https://doi.org/10.1021/ef502332k>
30. Koncsag, C., Tutun, I. A., Safta, C. (2011). Study of C5/C6 isomerization on Pt/H-zeolite catalyst in industrial conditions. *Chemistry*, 22(2), 102–106.
31. Smolikov, M. D., Kir'yanov, D. I., Shkurenok, V. A., Bikmetova, L. I., Belopukhov, E. A. et al. (2022). Integrated processes of the reforming and isomerization of gasoline fractions for the production of environmentally friendly motor gasolines. *Catalysis in Industry*, 14(3), 268–282. <https://doi.org/10.1134/S2070050422030035>
32. Du, Y., Feng, B., Jiang, Y., Yuan, L., Huang, K. et al. (2018). Solvent-free synthesis and *n*-hexadecane hydroisomerization performance of SAPO-11 catalyst. *European Journal of Inorganic Chemistry*, 2018(22), 2599–2606. <https://doi.org/10.1002/ejic.201800134>
33. Batalha, N., Astafan, A., Cavalcante, J., Reis, D., Pouilloux, Y. et al. (2015). Hydroisomerization of *n*-hexadecane over bifunctional Pt-HBEA catalysts. Influence of Si/Al ratio on activity selectivity. *Reaction Kinetics, Mechanisms and Catalysis*, 114(2), 661–673. <https://doi.org/10.1007/s11144-014-0794-z>
34. Tepin, H., Chayasari, S., Suchada, B., Resasco, D. E., Jongpatiwut, E. et al. (2018). Effect of metal-acid balance on hydroprocessed renewable jet fuel synthesis from hydrocracking and hydroisomerization of biohydrogenated diesel over Pt-supported catalysts. *Industrial & Engineering Chemistry Research*, 57(5), 1429–1440. <https://doi.org/10.1021/acs.iecr.7b04711>
35. Dhar, A., Vekariya, R. L., Bhadja, P. (2018). *n*-Alkane isomerization by catalysis—A method of industrial importance: An overview. *Cogent Chemistry*, 4(1), 1514686. <https://doi.org/10.1080/23312009.2018.1514686>
36. Samimi, A. (2021). New method of corrosion in isomerization units. *Advanced Journal of Chemistry—Section A*, 4(3), 206–219. <https://doi.org/10.22034/ajca.2021.277905.1248>
37. Torkaman, M., Kazemabadi, F. Z. (2017). The use of ethyl cellulose polymer to control drug release of hydrocortisone acetate. *Oriental Journal of Chemistry*, 33(4), 1976–1984. <https://doi.org/10.13005/ojc/330444>
38. He, S., Castello, D., Krishnamurthy, K. R., Al-Fatesh, A. S., Winkelman, G. M. et al. (2019). Kinetics of long chain *n*-paraffin dehydrogenation over a commercial Pt-Sn-K-Mg/ γ -Al₂O₃ catalyst: Model studies using *n*-dodecane. *Applied Catalysis A: General*, 579(5), 130–140. <https://doi.org/10.1016/j.apcata.2019.04.026>
39. Nestler, F., Müller, V. P., Ouda, M., Hadrich, M. J., Schaadt, A. et al. (2021). A novel approach for kinetic measurements in exothermic fixed bed reactors: Advancements in non-isothermal bed conditions demonstrated for methanol synthesis. *Reaction Chemistry and Engineering*, 6(6), 1092–1107. <https://doi.org/10.1039/D1RE00071C>
40. Parsafard, N., Asil, A. G., Mirzaei, S. (2021). Gas-phase catalytic isomerization of *n*-heptane using Pt/(CrO_x/ZrO₂)-HMS catalysts: A kinetic modeling. *International Journal of Chemical Kinetics*, 53(8), 971–981. <https://doi.org/10.1002/kin.21497>
41. Regali, F., Boutonnet, M., Järås, S. (2013). Hydrocracking of *n*-hexadecane on noble metal/silica-alumina catalysts. *Catalysis Today*, 214, 12–18. <https://doi.org/10.1016/j.cattod.2012.10.019>
42. Ancheyta, J. J., Villafuerte, M. E. (2000). Kinetic modeling of naphtha catalytic reforming reactions. *Journal of Energy & Fuels*, 14(5), 1032–1037. <https://doi.org/10.1021/ef0000274>
43. Khlebnikova, E., Bekker, A., Ivashkina, E. (2014). Hydrodynamics of reactant mixing in benzene with ethylene alkylation. *Procedia Chemistry*, 10(2), 297–304. <https://doi.org/10.1016/j.proche.2014.10.050>

44. Chekantsev, N. V., Gyngazova, M. S., Ivanchina, E. D. (2014). Mathematical modeling of light naphtha (C5, C6) isomerization process. *Chemical Engineering Journal*, 238(2), 120–128. <https://doi.org/10.1016/j.cej.2013.08.088>
45. Nikolaou, N., Papadopoulos, C. E., Gaglias, I. A., Pitarakis, K. G. (2004). A new non-linear calculation method of isomerization gasoline research octane number based on gas chromatographic data. *Fuel*, 83(4–5), 517–523. <https://doi.org/10.1016/j.fuel.2003.09.011>
46. Yasakova, E. A., Sitdikova, A. V., Achmetov, A. F. (2010). Tendency of isomerization process development in Russia and foreign countries. *Oil and Gas Business*, 1, 1–7. <https://www.elibrary.ru/item.asp?id=15263208>
47. Shehata, W. M., Mohamed, M. F., Fatma Khalifa Gad, F. K. (2018). Monitoring and modelling of variables affecting isomerate octane number produced from an industrial isomerization process. *Egyptian Journal of Petroleum*, 27(4), 945–953. <https://doi.org/10.1016/j.ejpe.2018.02.006>
48. Awan, Z. H., Kazmi, B., Hashmi, S., Raza, F., Hasan, S. et al. (2021). Process system engineering (PSE) analysis on process and optimization of the isomerization process. *Iranian Journal of Chemistry and Chemical Engineering*, 40(1), 289–302. https://ijcce.ac.ir/article_37243_e6e3d35b45ac5c57938d6df610752cfb.pdf
49. Chen, Z., Xu, J., Fan, Y., Shi, G., Bao, X. (2015). Reaction mechanism and kinetic modeling of hydroisomerization and hydroaromatization of fluid catalytic cracking naphtha. *Fuel Processing Technology*, 130, 117–126. <https://doi.org/10.1016/j.fuproc.2014.09.037>